Journal of Information Systems Engineering and Management
2026, 11(3s)
e-ISSN: 2468-4376
https://www.jisem-journal.com/

Research Article

An Advanced Lateral Control System Based on Multi-Machine Control for a Four-Wheel-Drive Electric Vehicle

Lachi Brahim[1], Berkani Abderrahmane[2], Negadi Karim[3], Aouadj Norediene[4]
[123] *Department of Electrical Engineering, Faculty of Applied sciences, Universitas IBN Khaldoun of Tiaret, Algeria*
[4]*Higher School in electrical and energy engineering (ESGEE), second cycle department, Oran, Algeria*

ARTICLE INFO

Received: 30 Dec 2024
Revised: 12 Feb 2025
Accepted: 26 Feb 2025

ABSTRACT

Introduction: Traditional mechanical differentials in four-wheel-drive (4WD) vehicles distribute torque passively and symmetrically, which limits their ability to adapt to varying road conditions. This limitation negatively affects lateral stability and vehicle maneuverability, especially during high-speed cornering and low-traction scenarios.

Objectives: This study aims to develop an advanced lateral control strategy for 4WD electric vehicles by replacing the conventional mechanical differential with a controllable electric differential, in order to enhance vehicle stability, handling, and safety.

Methods: The proposed approach is based on multi-machine control, where each wheel is driven by an independent electric motor supplied by two synchronized three-level Neutral Point Clamped (NPC) inverters. This configuration enables precise and real-time torque distribution among the wheels. An electric differential control algorithm is implemented to actively regulate wheel torques, ensuring proper yaw rate and lateral force control under varying driving conditions.

Results: The effectiveness of the proposed system is validated through numerical simulations under critical driving conditions, including sudden steering inputs and low-adhesion surfaces. The results demonstrate improved lateral stability, reduced trajectory deviation, and strong robustness of the control strategy.

Conclusions: The study confirms that electric differential-based control is a promising solution for next-generation electric vehicles. It significantly enhances vehicle handling, agility, and safety by enabling adaptive and intelligent torque distribution.

Keywords: Electric vehicle, Four-wheel-drive, In-wheels motors, Master-slave, Lateral control, Electric differential.

INTRODUCTION

In recent years, the rapid advancement of electric vehicle (EV) technologies has sparked significant interest in the research and development of high-performance, energy-efficient propulsion systems. As the automotive industry transitions away from internal combustion engines toward more sustainable mobility solutions, electric traction motor technologies have become central to this innovation [1-3]. This shift has led to the development and deployment of advanced motor architectures designed for variable-speed applications in EVs. Notably, Permanent Magnet Synchronous Motors (PMSMs) have emerged as a preferred choice due to their high efficiency, superior power density, and precise control characteristics [1], [4-6]. Induction Motors (IMs) are also widely used due to their robustness, tolerance to harsh conditions, and well-established control techniques, and are prominent in high-performance cars [7]. Another alternative, Switched Reluctance Motors (SRMs), offers a rugged and fault-tolerant design with low manufacturing costs. Recent advances in SRM topology—such as hybrid-excited and optimized tooth structures—have greatly improved their torque density and efficiency, making them stronger competitors in EV traction [8]. Meanwhile, Axial Flux Motors are gaining ground in next-generation propulsion applications due to their compactness, exceptionally high torque-to-weight ratio, and overall power density.

Journal of Information Systems Engineering and Management
2026, 11(3s)
e-ISSN: 2468-4376
https://www.jisem-journal.com/

Research Article

Traction motors in electric vehicles (EVs) face unique challenges compared to industrial motors, which typically operate under steady-state conditions. Due to the dynamic nature of vehicle movement, EV traction motors must handle highly variable operating conditions, requiring advanced design and control strategies [9]. One key challenge is the need for frequent starts, stops, and rapid acceleration, particularly in urban driving environments. High efficiency at low speeds and precise torque control are essential for smooth acceleration and deceleration, while regenerative braking plays a crucial role in improving overall efficiency by recovering energy during braking [10, 11]. Additionally, EV traction motors must meet specific torque demands in different driving scenarios. Hill climbing requires high torque at low speed, necessitating strong torque capabilities without excessive heating or efficiency losses. Conversely, high-speed cruising demands low torque at high speed, meaning the motor must maintain efficiency while minimizing energy losses [12]. Another critical aspect is fast and robust torque response, as EV motors must react instantly to driver input, unlike industrial motors that experience gradual load variations. This requires advanced control techniques such as Field-Oriented Control (FOC) or Direct Torque Control (DTC) to ensure quick and accurate torque adjustments [13, 14]. Furthermore, minimizing torque ripple is essential for vehicle comfort and noise reduction. Torque ripple, which refers to fluctuations in motor torque, can cause mechanical vibrations and noise. To maintain torque ripple within ±2%, advanced motor control algorithms and precise motor design (including optimized rotor and stator geometry) are necessary [14, 15]. A smooth torque profile enhances passenger comfort, reduces mechanical stress, and extends the vehicle's lifespan. These factors highlight the complexity of EV traction motor design and the need for continuous advancements in motor control, efficiency, and performance. Direct Torque Control (DTC) for Permanent Magnet Synchronous Motor (PMSM) drives has gained significant attention in industrial motor applications due to its advantages and practical implementation in electric vehicles (EVs) [16, 17].

The use of multiple electric actuators is often necessary due to size and power limitations of a single actuator or the need for independent control of multiple components. This approach enhances system efficiency, flexibility, and precision, making it ideal for applications in robotics, industrial automation, and electric traction [18] [19]. Multi-converter multi-machine (SMM) systems, which integrate multiple electrical machines and static converters, are widely used in electromechanical applications. These systems offer improved efficiency, flexibility, and reliability, making them essential for industrial automation, transportation, and renewable energy. However, their complexity requires advanced control strategies for optimal performance [20] [21].

The multi-converter multi-machine (SMM) traction system is commonly used in electric vehicles (EVs), where each wheel is powered by an independent motor. This configuration enhances traction, stability, and energy efficiency, enabling independent four-wheel drive (4WD). However, it requires advanced control strategies to manage power distribution and synchronization effectively. Despite its complexity and cost, SMM traction systems are promising for the future of electric mobility [22, 23]. This study aims to ensure independent control of each wheel motor by adopting a multi-motor solution in the traction system architecture of an electric vehicle. In multi-machine systems, such as four-wheel-drive (4WD) electric vehicles with in-wheel motors, proper control strategies are essential to manage torque distribution, energy efficiency, and coupling effects between multiple motors. Several control structures have been developed to optimize performance, including independent machine control, average control, and master-slave control [8, 20, 21, 24]. A possible solution to this issue is to employ a master-slave control structure for each pair of side drive wheels, driven by two permanent magnet synchronous motors that are supplied in parallel by a three-phase, three-level NPC inverter.

This work aims to advance the study and enhancement of the lateral dynamics of a traction system regulated by a robust "master-slave" control structure based on Direct Torque Control (DTC). The goal is to implement an electric differential that ensures speed synchronization of the drive wheels during motion, thereby improving the stability and safety of the four-wheel-drive electric vehicle. The article is structured as follows: Section 1 introduces the configuration of the traction system of the studied electric vehicle, where a permanent magnet synchronous motor (PMSM) is selected as the traction motor. This section also details the mathematical model of the PMSM along with the dynamic model of the EV. The traction system under study consists of four PMSMs driving the four-wheel drive, with each pair of motors powered by a single three-phase, three-level NPC inverter. Section 3 discusses the multi-machine control structure implemented for the lateral control of the four-wheel-drive electric vehicle. Specifically, a

Journal of Information Systems Engineering and Management
2026, 11(3s)
e-ISSN: 2468-4376
https://www.jisem-journal.com/

Research Article

master-slave control strategy based on Direct Torque Control (DTC) is applied to a dual-motor traction system powered by a single inverter. Section 4 focuses on the lateral behavior analysis of the four-wheel-drive electric vehicle. The proposed control structure is implemented and tested through simulations to evaluate its robustness, particularly in critical cornering situations. Finally, the conclusions are presented in Section 5.

CONFIGURATION OF 4WD ELECTRIC VEHICLE

Figure 1 shows the architecture of a four-wheel-drive (4WD) electric vehicle (EV) equipped with four in-wheel permanent magnet synchronous motors (PMSMs), where each wheel is driven independently. This configuration enables precise torque control for each wheel, significantly enhancing vehicle stability and maneuverability. The system is powered by a central battery pack and controlled through two synchronized three-phase inverters, with each inverter managing a pair of motors. This configuration enhances efficiency, torque control, and system reliability, making it well-suited for high-performance EV applications [25] [26]. We assume that the two driving wheels on the front axle (M1 and M3) and the rear axle (M2 and M4) are what propel this vehicle. The objective of the structure under study is to replicate the operation of a differential mechanism by successively adding safety functions [27] [28].

MATHEMATICAL MODEL OF PMSM

The mathematical model of a Permanent Magnet Synchronous Motor (PMSM) can be written in the $\alpha\beta$ reference frame using the following equations [27] :

Voltage equations :

$$v_\alpha = R_s i_\alpha + L_s \frac{di_\alpha}{dt} - \omega_m \Phi_f \sin\theta$$
$$v_\beta = R_s i_\beta + L_s \frac{di_\beta}{dt} + \omega_m \Phi_f \cos\theta \quad (1)$$

Where Φ_α is the α -axis flux linkage and Φ_β is the β -axis flux linkage, which can be expressed as follow :

$$\Phi_\alpha = L_s i_\alpha + \Phi_f \cos\theta$$
$$\Phi_\beta = L_s i_\beta + \Phi_f \sin\theta \quad (2)$$

Electromagnétique torque :

$$T_{em} = \frac{3}{2} p\left(\Phi_\alpha i_\beta - \Phi_\beta i_\alpha\right) \quad (3)$$

The electromechanical equation is expressed by:

$$J \frac{d\omega_m}{dt} + T_{friction} = T_e - T_{load} \quad (4)$$

Where, T_{load} is the load torque, $T_{friction}$ is the motor-load system friction torque, and J is the polar moment of inertia of the rotor and the connected load.

This model is fundamental for the control and simulation of PMSM drives, especially in electric vehicle applications where precise torque and speed control are required.

Journal of Information Systems Engineering and Management
2026, 11(3s)
e-ISSN: 2468-4376
https://www.jisem-journal.com/

Research Article

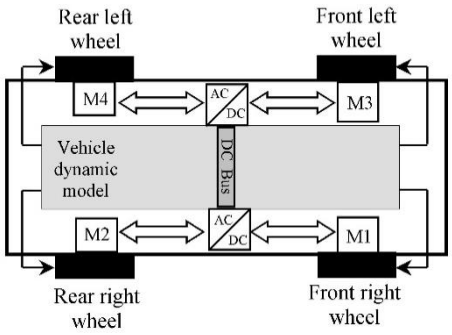

Figure 1. Structure of the 4WD electric vehicle under study.

VEHICLE DYNAMIC MODEL

The dynamic model of a four-wheel drive (4WD) electric vehicle (EV) describes the longitudinal, lateral, and yaw dynamics of the vehicle based on Newton's laws of motion. It is essential for stability control, trajectory tracking, and torque distribution. The equations of longitudinal, lateral, and yawing motion of vehicle are given by [29]:

$$\begin{aligned} M_v(\dot{v}_x - rv_y) &= \sum_{i=1}^{4} F_{xi}\cos\delta_i - \sum_{i=1}^{4} F_{yi}\sin\delta_i - 0{,}5\rho S_f C_{px} v_x^2 - M_v g\sin\alpha_p \\ M_v(\dot{v}_x + rv_y) &= \sum_{i=1}^{4} F_{xi}\sin\delta_i + \sum_{i=1}^{4} F_{yi}\cos\delta_i - 0{,}5\rho S_f C_{px} v_x^2 - M_v g\sin\alpha_p \\ J_v\dot{r} &= \sum_{i=1}^{4} F_{xi}\sin\delta_i x_i + \sum_{i=1}^{4} F_{yi}\cos\delta_i x_i - \sum_{i=1}^{4} F_{xi}\cos\delta_i y_i + \sum_{i=1}^{4} F_{xi}\sin\delta_i y_i + \sum_{i=1}^{4} M_{ai} + 0{,}5\rho S_f C_{px} v_x^2 \end{aligned} \tag{5}$$

The sideslip angle (or slip angle) is a key parameter in vehicle dynamics, affecting handling, stability, and control. It represents the difference between the direction of the wheel's motion and the actual direction the tire is pointing. The sideslip angle for the front and rear wheels is as follows:

$$\begin{cases} \alpha_1 = \arctan\left(\dfrac{1}{V_x + d}\left(V_y + rL_f\right)\right) - \delta \\ \alpha_3 = \arctan\left(\dfrac{1}{V_x - d}\left(V_y + rL_f\right)\right) - \delta \\ \alpha_2 = \arctan\left(\dfrac{1}{V_x - d}\left(V_y + rL_r\right)\right) \\ \alpha_4 = \arctan\left(\dfrac{1}{V_x - d}\left(V_y + rL_r\right)\right) \end{cases} \tag{6}$$

The longitudinal adhesion coefficient μ_a (or longitudinal friction coefficient) represents the ratio between the tangential (traction or braking) force exerted by a tire and the normal force acting on it. It plays a crucial role in vehicle traction, braking, and acceleration dynamics. It is defined as:

$$\mu_a = \frac{F_x}{F_z} \tag{7}$$

The slip ratio measures the difference between the wheel speed and the actual vehicle speed:

$$\lambda = \frac{v_x - R\omega_m}{v_x} \tag{8}$$

The rear and front axle loads acting on the wheel contact points can be simplified as follows:

Journal of Information Systems Engineering and Management
2026, 11(3s)
e-ISSN: 2468-4376
https://www.jisem-journal.com/

Research Article

$$
\begin{aligned}
F_{z1} &= \frac{L_r g M_v}{2L} - \frac{h_{cg} M_v}{2L}(\dot{V}_x - rV_y) + \frac{h_{cg} M_v}{2l_w}(\dot{V}_y + rV_x) \\
F_{z3} &= \frac{L_r g M_v}{2L} - \frac{h_{cg} M_v}{2L}(\dot{V}_x - rV_y) - \frac{h_{cg} M_v}{2l_w}(\dot{V}_y + rV_x) \\
F_{z2} &= \frac{L_f g M_v}{2L} - \frac{h_{cg} M_v}{2L}(\dot{V}_x - rV_y) + \frac{h_{cg} M_v}{2l_w}(\dot{V}_y + rV_x) \\
F_{z4} &= \frac{L_f g M_v}{2L} - \frac{h_{cg} M_v}{2L}(\dot{V}_x - rV_y) - \frac{h_{cg} M_v}{2l_w}(\dot{V}_y + rV_x)
\end{aligned} \tag{9}
$$

The linear speeds for the four wheels can be written as :

$$
\begin{aligned}
u_{t1} &= (v_x + dr)\cos\delta + (v_y + l_f r)\sin\delta \\
u_{t2} &= v_x + dr \\
u_{t3} &= (v_x - dr)\cos\delta + (v_y + l_r r)\sin\delta \\
u_{t4} &= v_x - dr
\end{aligned} \tag{10}
$$

PROPOSED MULTI-MACHINE CONTROL FOR LATERAL CONTROL OF 4WD ELECTRIC VEHICLE

DTC is an effective control method for PMSM and Induction Motors in EVs, offering fast and precise torque and flux regulation by adjusting the stator flux. Its efficiency and responsiveness make it ideal for high-performance traction applications. In the Direct Torque Control (DTC) of two motors driven by a single inverter, there are two feedback loops: one for controlling the stator flux and the other for the electromagnetic torque. Moreover, the proposed method also uses both control loops but with different procedures in each loop. Figure 2 shows the diagram of multi-machine control structure applied for lateral control of electric four-wheel drive vehicle.

When two motors are driven by a single inverter, the control strategy becomes more complex, requiring advanced techniques to ensure independent control of each motor's torque and flux. In a traditional DTC scheme, a single inverter is responsible for controlling one motor by adjusting its torque and flux. However, in a system with two motors driven by a single inverter, the inverter must generate appropriate voltage vectors to satisfy the torque and flux requirements of both motors simultaneously. Since the inverter has only three output phases, both motors must share these phases, which leads to interaction and coupling effects between the motors.

To ensure independent control of both motors, the proposed DTC scheme modifies the traditional control approach by:

- Using separate flux and torque control loops for each motor
- Implementing priority-based voltage vector selection
- Using a modified switching table to ensure optimal voltage vector distribution between the two motors
- Reducing torque ripple by optimizing hysteresis band selection

These modifications enable better dynamic performance, minimize interaction effects, and improve overall system efficiency.

ELECTROMAGNETIC TORQUE CONTROL LOOP

The torque control loop's novel concept is to calculate the system's requirements while accounting for the torques of the two motors. This is made possible by an equivalent table that will be generated for the torque control loop situation that uses a five-level comparator [30]. The various scenarios for the "H_{Te}" torque error in the control loop based on the five-level comparators' outputs are detailed in Table 1.

Journal of Information Systems Engineering and Management
2026, 11(3s)
e-ISSN: 2468-4376
https://www.jisem-journal.com/

Research Article

Table 1. Torque lookup table.

		Motor 2				
	H_{T_e}	**-2**	**-1**	**0**	**1**	**2**
Motor 1	**-2**	-2	-1	-2	-1	0
	-1	-1	-1	-1	0	1
	0	-2	-1	0	1	0
	1	-1	0	1	1	1
	2	0	1	2	1	2

STATOR FLUX CONTROL LOOP

In the stator flux control loop, it is essential to ensure that the flux in any machine does not exceed its nominal value. In the proposed method, a "master-slave" switching strategy is implemented to regulate the stator flux. To accurately select the master motor and prevent flux saturation, the motor with the least torque is designated as the master. Finally, the appropriate voltage vector is selected using the classic DTC selection table (Table 2), based on the outputs from Table 1 and the stator flux control loop.

In the overall control architecture of the four-wheel-drive electric vehicle, illustrated in Figure 2, the electric differential block plays a pivotal role. Its primary function is to compute and assign individual speed references to each in-wheel motor, thereby enabling optimal torque distribution and enhancing vehicle performance under various driving conditions.

To fulfill this function, the electric differential relies on a comprehensive set of real-time data acquired from multiple onboard sensors. These include, but are not limited to :

The longitudinal speed of the vehicle (typically obtained from GPS or wheel encoders),

The steering wheel angle, which reflects the driver's intended trajectory and allows estimation of the turning radius,

Using these inputs, the electric differential determines the appropriate angular velocity for each wheel. For example, during cornering, it commands a slightly higher speed to the outer wheels compared to the inner ones, effectively emulating the behavior of a conventional mechanical differential while benefiting from the precision and flexibility of electric control.

The resulting wheel speeds and their differences are governed by geometric and kinematic relations, which can be expressed through specific mathematical equations.

In the general diagram shown in Figure 2, the electric differential provide the speed references for each two-motor, as well as their difference are expressed by :

$$\omega_{r\_l} = \frac{L_w + d_w / 2.\tan\delta}{L_\omega}\omega_v$$
$$\omega_{r\_R} = \frac{L_w - d_w / 2.\tan\delta}{L_\omega}\omega_v \quad (11)$$

And the difference in speed between the right and left driving wheels is written:

$$\Delta\omega = \omega_{r\_l} - \omega_{r\_r} = \frac{d_\omega tan\delta}{L_w}\omega_v \quad (12)$$

This equation expresses the difference in rotational speeds between the left and right drive wheels as a function of the steering angle, wheelbase, and vehicle speed:

Journal of Information Systems Engineering and Management
2026, 11(3s)
e-ISSN: 2468-4376
https://www.jisem-journal.com/

Research Article

- ω_{r_l}, ω_{r_R} : rotational speeds of the left and right wheels, respectively.
- $\Delta\omega$: speed difference between left and right wheels.
- $d\omega$: lateral distance between the two drive wheels (track width).
- $\Delta\omega$: steering angle of the front wheels (provided by a steering angle sensor).
- L_ω : wheelbase of the vehicle (distance between front and rear axles).
- ω_v : vehicle's reference angular speed (derived from linear speed and wheel radius).

The steering wheel steering angle can be expressed by:

$$\begin{cases} \delta > 0 \; for \; a \; \text{right turn} \\ \delta < 0 \; for \; a \; left \; \text{turn} \\ \delta = 0 \; when \; the \; vehicle \; is \; moving \; \text{straight ahead} \end{cases}$$

(13)

The steering wheel angle δ\deltaδ indicates the vehicle's intended direction.

- In a right turn: the right wheels rotate more slowly, while the left wheels rotate faster.
- In a left turn: the left wheels rotate more slowly, while the right wheels rotate faster.
- In straight-line motion: all wheels rotate at approximately the same speed.

The electric differential uses δ\deltaδ to adjust wheel speeds dynamically, ensuring smooth cornering, optimal torque distribution, and enhanced stability and comfort.

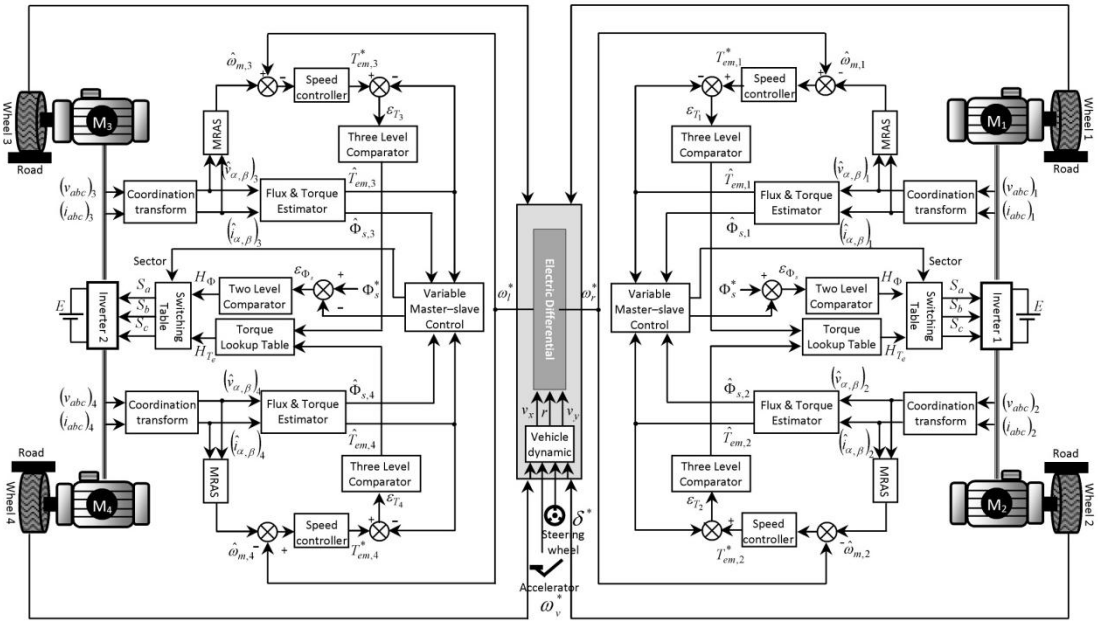

Figure 2. Block diagram of the multi-machine control structure applied for lateral control of a 4WD-EV.

Journal of Information Systems Engineering and Management
2026, 11(3s)
e-ISSN: 2468-4376
https://www.jisem-journal.com/

Research Article

Table 2. DTC selection table for driving andriven by a 3-level NPC inverter.

τ_Φ	τ_T	Stator flux sector											
		1	2	3	4	5	6	7	8	9	10	11	12
+1	+2	$\vec{V}_2$	$\vec{V}_3$	$\vec{V}_4$	$\vec{V}_5$	$\vec{V}_6$	$\vec{V}_7$	$\vec{V}_8$	$\vec{V}_9$	$\vec{V}_{10}$	$\vec{V}_{11}$	$\vec{V}_{12}$	$\vec{V}_1$
	+1	$\vec{V}_2$	$\vec{V}_{15}$	$\vec{V}_4$	$\vec{V}_{17}$	$\vec{V}_6$	$\vec{V}_{19}$	$\vec{V}_8$	$\vec{V}_{21}$	$\vec{V}_{10}$	$\vec{V}_{23}$	$\vec{V}_{12}$	$\vec{V}_{13}$
	0	$\vec{V}_{25}$	$\vec{V}_{26}$	$\vec{V}_{27}$	$\vec{V}_{25}$	$\vec{V}_{26}$	$\vec{V}_{27}$	$\vec{V}_{25}$	$\vec{V}_{26}$	$\vec{V}_{27}$	$\vec{V}_{25}$	$\vec{V}_{26}$	$\vec{V}_{27}$
	-1	$\vec{V}_{12}$	$\vec{V}_{13}$	$\vec{V}_2$	$\vec{V}_{15}$	$\vec{V}_4$	$\vec{V}_{17}$	$\vec{V}_6$	$\vec{V}_{19}$	$\vec{V}_8$	$\vec{V}_{21}$	$\vec{V}_{10}$	$\vec{V}_{23}$
	-2	$\vec{V}_{12}$	$\vec{V}_1$	$\vec{V}_2$	$\vec{V}_3$	$\vec{V}_4$	$\vec{V}_5$	$\vec{V}_6$	$\vec{V}_7$	$\vec{V}_8$	$\vec{V}_9$	$\vec{V}_{10}$	$\vec{V}_{11}$
0	+2	$\vec{V}_4$	$\vec{V}_5$	$\vec{V}_6$	$\vec{V}_7$	$\vec{V}_8$	$\vec{V}_9$	$\vec{V}_{10}$	$\vec{V}_{11}$	$\vec{V}_{12}$	$\vec{V}_1$	$\vec{V}_2$	$\vec{V}_3$
	+1	$\vec{V}_4$	$\vec{V}_{17}$	$\vec{V}_6$	$\vec{V}_{19}$	$\vec{V}_8$	$\vec{V}_9$	$\vec{V}_{10}$	$\vec{V}_{11}$	$\vec{V}_{12}$	$\vec{V}_1$	$\vec{V}_2$	$\vec{V}_3$
	0	$\vec{V}_{25}$	$\vec{V}_{26}$	$\vec{V}_{27}$	$\vec{V}_{25}$	$\vec{V}_{26}$	$\vec{V}_{27}$	$\vec{V}_{25}$	$\vec{V}_{26}$	$\vec{V}_{27}$	$\vec{V}_{25}$	$\vec{V}_{26}$	$\vec{V}_{27}$
	-1	$\vec{V}_{10}$	$\vec{V}_{23}$	$\vec{V}_{12}$	$\vec{V}_{13}$	$\vec{V}_2$	$\vec{V}_{15}$	$\vec{V}_{10}$	$\vec{V}_{17}$	$\vec{V}_6$	$\vec{V}_{19}$	$\vec{V}_8$	$\vec{V}_{21}$
	-2	$\vec{V}_{10}$	$\vec{V}_{11}$	$\vec{V}_{12}$	$\vec{V}_1$	$\vec{V}_2$	$\vec{V}_3$	$\vec{V}_4$	$\vec{V}_5$	$\vec{V}_6$	$\vec{V}_7$	$\vec{V}_8$	$\vec{V}_9$
-1	+2	$\vec{V}_5$	$\vec{V}_6$	$\vec{V}_7$	$\vec{V}_8$	$\vec{V}_9$	$\vec{V}_{10}$	$\vec{V}_{11}$	$\vec{V}_{12}$	$\vec{V}_1$	$\vec{V}_2$	$\vec{V}_3$	$\vec{V}_4$
	+1	$\vec{V}_{17}$	$\vec{V}_6$	$\vec{V}_{19}$	$\vec{V}_8$	$\vec{V}_{21}$	$\vec{V}_{10}$	$\vec{V}_{23}$	$\vec{V}_{12}$	$\vec{V}_{13}$	$\vec{V}_2$	$\vec{V}_{15}$	$\vec{V}_4$
	0	$\vec{V}_{25}$	$\vec{V}_{26}$	$\vec{V}_{27}$	$\vec{V}_{25}$	$\vec{V}_{26}$	$\vec{V}_{27}$	$\vec{V}_{25}$	$\vec{V}_{26}$	$\vec{V}_{27}$	$\vec{V}_{25}$	$\vec{V}_{26}$	$\vec{V}_{27}$
	-1	$\vec{V}_{21}$	$\vec{V}_{10}$	$\vec{V}_{23}$	$\vec{V}_{12}$	$\vec{V}_{13}$	$\vec{V}_2$	$\vec{V}_{15}$	$\vec{V}_4$	$\vec{V}_{17}$	$\vec{V}_6$	$\vec{V}_{19}$	$\vec{V}_8$
	-2	$\vec{V}_9$	$\vec{V}_{10}$	$\vec{V}_{11}$	$\vec{V}_{12}$	$\vec{V}_1$	$\vec{V}_2$	$\vec{V}_3$	$\vec{V}_4$	$\vec{V}_5$	$\vec{V}_6$	$\vec{V}_7$	$\vec{V}_8$

To ensure the stability of the system composed of two PMSMs connected in parallel and controlled by a single inverter using a master-slave DTC structure, various load conditions are applied to both machines, as illustrated in Figure3(a). The simulation results clearly show that the system remains stable regardless of the torque values delivered by the two machines. The master motor is identified as the one delivering the higher torque, and the relative position difference between the two machines aligns with theoretical expectations—particularly when PMSM1 acts as the master. Moreover, Figure 3(a) illustrates the electromagnetic torque profiles of the two machines. It can be observed that they accurately track the variations in the applied load torques, with a fast transient response, free from prolonged oscillations or significant overshoot. This effective tracking of the load torques confirms the efficiency of the Direct Torque Control (DTC) strategy in maintaining robust dynamic performance even in the presence of mechanical disturbances. In addition, Figures 3(b) and 3(c) show the stator flux trajectories of the two machines. These remain generally stable and maintain a nearly circular shape, unaffected by the successive changes in applied load. This stability confirms the decoupling between flux and torque control—an essential property of DTC—ensuring robust flux regulation regardless of mechanical disturbances.

This approach significantly contributes to the reduction of both torque ripples and flux oscillations, thereby improving the precision of torque control and enhancing the overall stability and robustness of the system. Overall, the simulation results demonstrate the effectiveness of the proposed control strategy in ensuring fast dynamic response, reduced steady-state error, and improved performance under varying load conditions.

Journal of Information Systems Engineering and Management
2026, 11(3s)
e-ISSN: 2468-4376
https://www.jisem-journal.com/

Research Article

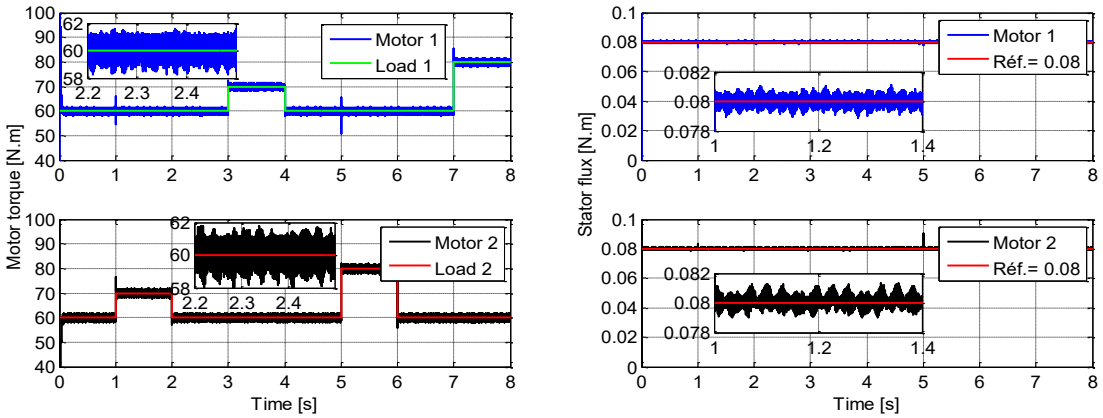

(a) (b)

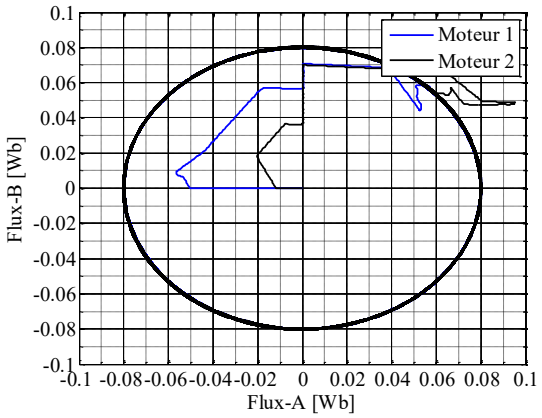

(c)

Figure 3. Simulation Results of the Master-Slave DTC Control.

SIMULATION RESULTS AND DISCUSSION

This section presents simulation results using Matlab/Simulink to demonstrate the enhanced lateral stability of an electric vehicle equipped with four in-wheel motors during various turning maneuvers. Table 4 provides the specifications of the PMSMs, while Table 5 summarizes the numerical values of the studied electric vehicle.

Table 4. Motor parameters.

Symbol	Quantity	Value
R_s	resistance	0,03 Ω
L_d	d-axis inductance	0,2 mH
L_q	q-axis inductance	0,2 mH
Φ_f	permanent magnet flux	0,08 Wb
p	pole pairs	4

Journal of Information Systems Engineering and Management
2026, 11(3s)
e-ISSN: 2468-4376
https://www.jisem-journal.com/

Research Article

Table 5. Electric vehicle parameters.

Symbol	Quantity	Value
M_v	vehicle mass	1562 kg
J_v	vehicle inertia	2630 kg.m²
J_ω	wheel inertia	1,284 kg.m²
L_f	distance from the CG to front axle	1,104 m
L_r	distance from the CG to rear axle	1,421 m
h_{cg}	heigh of the vehicle ctroid (CG)	0,5 m
S_f	frontal area of vehicle	2,04 m²
ρ	air density	1,2 kg.m^{-3}
C_{px}	drag coefficient	0,25
C_{rr}	rolling resistance coefficient	0,01
C_f	longitudinal stiffness of each tire lateral	37407 N/rad
C_r	lateral stiffness of each tire lateral	51918 N/rad
R_ω	wheel radius	0,294 m

To better understand the operation of the traction system in a four-wheel-drive electric vehicle controlled by a master-slave Direct Torque Control (DTC) strategy, a realistic dynamic scenario was simulated. In this scenario, the vehicle follows a sequence of tight right and left turns, accurately replicating real-world driving conditions typically encountered on winding roads or in dense urban environments. The vehicle moves at a constant speed while tracking a predefined steering angle profile, applied to the front steering wheels, which defines the trajectory geometry. These rapid directional changes induce significant variations in vertical load, longitudinal speed, lateral acceleration, and traction forces on each driving wheel. A detailed analysis of these variables allows for the identification of several key physical and control-related phenomena, thereby offering valuable insights into the performance and robustness of the proposed control strategy.

In this simulation, the four-wheel-drive electric vehicle is capable of performing a sequence of turns according to the road geometry, with gradual variations in the steering angle as defined in Figure 4(a). The steering angle is adjusted according to the different phases of each turn. Figure 4(b) illustrates the accurate tracking of the vehicle's linear velocity. This result indicates that the vehicle is able to precisely follow the reference speed imposed during the simulation, despite the dynamic variations induced by successive turning maneuvers. The close alignment between the actual and reference velocities highlights the effectiveness of the control system in maintaining speed stability. It also confirms that the traction system, along with the master-slave DTC strategy, successfully compensates for disturbances caused by load transfers, steering angle variations, and changes in traction demand during cornering. Such precise velocity tracking is crucial for ensuring both driving comfort and control accuracy under dynamic driving conditions.

Journal of Information Systems Engineering and Management
2026, 11(3s)
e-ISSN: 2468-4376
https://www.jisem-journal.com/

Research Article

When a vehicle enters a turn, it experiences a centrifugal force directed outward from the curve, which is proportional to its speed and the curvature radius of the trajectory. This force acts on the vehicle's center of gravity (CG), resulting in a lateral load transfer. As a consequence, the vertical load (or normal force) on the wheels located on the outside of the turn increases, while it decreases on the inner wheels, as shown in Figure 4(c). This phenomenon alters the distribution of tire-road adhesion between the wheels, directly affecting the vehicle's stability and traction during cornering.

Electric motors, which enable precise, fast and independent torque control at each wheel, allow the lateral load transfer to be actively managed to simultaneously improve both traction and dynamic vehicle stability during cornering. Indeed, a wheel subjected to a higher vertical load can transmit a greater driving torque without the risk of slipping, in accordance with tire-road adhesion laws. Accordingly, an advanced control strategy—such as the master-slave Direct Torque Control (DTC)—enables a dynamic and optimized distribution of motor torque among the driving wheels. This approach allows the control system to intelligently allocate torque based on the vehicle's dynamic conditions during cornering (see Figure 4(d), which illustrates the motor torques). Specifically, the controller increases the torque applied to the outer wheels, which benefit from improved grip due to the greater vertical load induced by lateral mass transfer. Simultaneously, it reduces the torque on the inner wheels, which are more prone to slipping as a result of reduced load. This adaptive torque distribution not only enhances traction but also improves the vehicle's lateral stability and cornering performance.

When a four-wheel-drive electric vehicle enters a turn, each of its wheels follows a circular path with a different radius, resulting in varying rotational speeds between the inner and outer wheels. The outer wheels, covering a longer distance, must rotate at a higher speed than the inner wheels. This speed difference is critical to ensure smooth maneuvering, avoid undesired mechanical stresses in the drivetrain, and maintain vehicle stability. Thanks to the selected four-wheel-drive architecture, each electric motor can independently regulate the rotational speed of its corresponding wheel, under the coordination of a master-slave Direct Torque Control (DTC) strategy. This system simultaneously adjusts both torque and speed at each wheel to follow the correct kinematic trajectories, reduce internal mechanical constraints, and enhance vehicle stability during cornering. Figure 4(e) clearly illustrates the speed response of the four driving wheels under such conditions.

The traction forces are illustrated in Figure 4(f). On a straight, horizontal road with uniform grip conditions, the traction forces are typically balanced between the front and rear axles. During a left-hand turn, lateral load transfer occurs toward the right-hand wheels. These wheels, being more heavily loaded, benefit from greater vertical grip and can therefore support higher traction forces. In contrast, the inner (left-hand) wheels experience reduced loading, which limits their ability to transmit torque. The hybrid control strategy dynamically adjusts torque distribution to take full advantage of the maximum available grip on the most loaded wheels. In a right-hand turn, the phenomenon is symmetrical: the load shifts to the left-hand wheels, which then become the primary contributors to traction, while the right-hand wheels offer reduced capacity. Optimized management of motor torque—achieved through the implemented master-slave DTC strategy—thus ensures that both vehicle traction and stability are maintained, regardless of the turn direction.

Figure 4(g) shows the evolution of the vehicle's longitudinal speed. On a straight path, this speed is positive and generally high, as the vehicle moves freely along its chassis axis. During cornering, Vx slightly decreases compared to straight-line motion. This reduction is due to additional forces associated with steering input and the presence of lateral forces, which influence the motion and slightly reduce forward speed. The tighter the turn, the more noticeable this decrease becomes.

During straight-line motion, the vehicle's lateral velocity is zero or remains very close to zero, indicating the absence of lateral displacement. In contrast, during cornering, the vehicle's lateral velocity takes on a non-zero value: it becomes positive during a left turn and negative during a right turn (see Figure 4(h)). This variation reflects the lateral displacement of the vehicle's center of gravity induced by the curved trajectory.

Regarding the yaw rate, which represents the vehicle's rotational speed around its vertical axis, it is zero during straight-line motion, as the vehicle is not turning. However, it becomes positive during a left turn and negative during a right turn (see Figure 4(i)). The transient observed on the yaw rate curve corresponds to the vehicle's dynamic

Journal of Information Systems Engineering and Management
2026, 11(3s)
e-ISSN: 2468-4376
https://www.jisem-journal.com/

Research Article

adaptation period between a straight and a curved trajectory. During this phase, the yaw rate evolves progressively (increasing or decreasing) until it reaches a steady-state value specific to the initiated turn. This behavior reflects the dynamic response of a system with inertia, in which the effects of steering do not occur instantaneously but with a delay related to the vehicle's mechanical and dynamic properties.

Lateral forces take positive values when directed to the right, and negative values when pointing to the left, as illustrated in Figure 4(j). Thus, during a right turn, the vehicle experiences a centrifugal force directed outward, which the tires must counteract by generating a lateral force oriented inward, i.e., toward the right side of the vehicle — resulting in positive lateral forces. Conversely, during a left turn, the tires produce a lateral force directed to the left to oppose skidding, which, in the same reference frame, corresponds to a negative lateral force.

An electric differential enhances vehicle dynamics in turns by improving stability, preventing wheel slip, and optimizing cornering performance. It ensures better traction by distributing torque to each wheel based on grip conditions, maximizing control and minimizing power losses. This increased efficiency leads to better energy utilization, while precise wheel speed management enhances handling, resulting in smoother and more responsive turns.

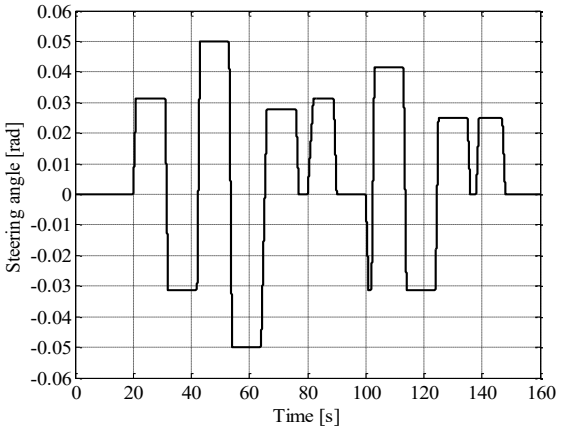

(a) Steering angle input

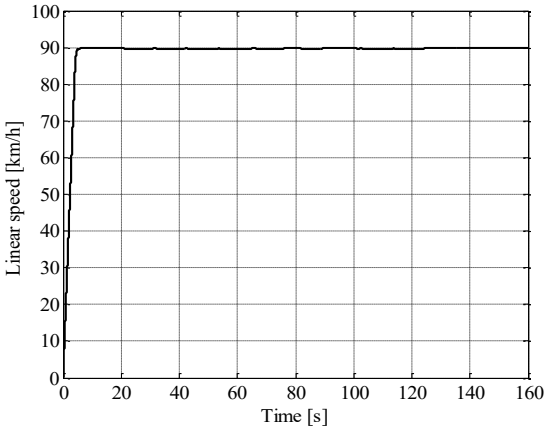

(b) Linear speed of the vehicle

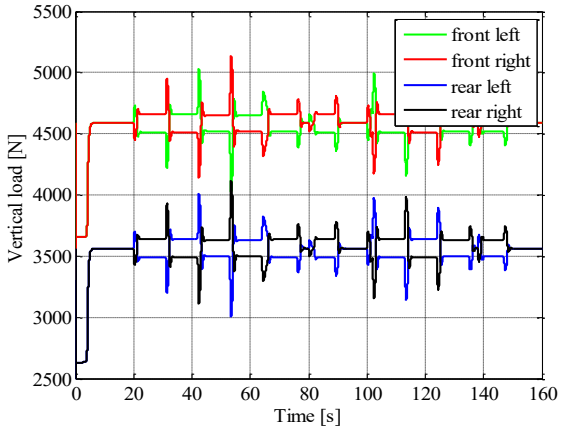

(c) Vertical load

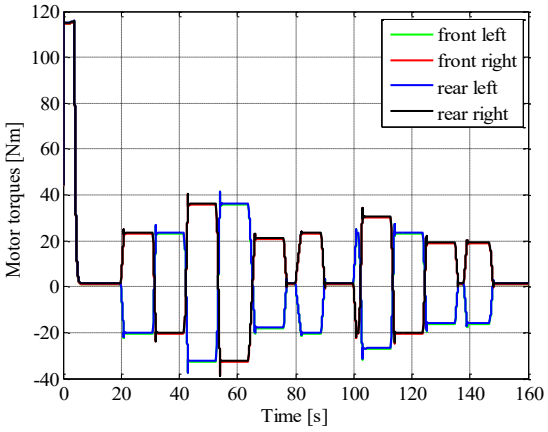

(d) Torque of motors

Journal of Information Systems Engineering and Management
2026, 11(3s)
e-ISSN: 2468-4376
https://www.jisem-journal.com/

Research Article

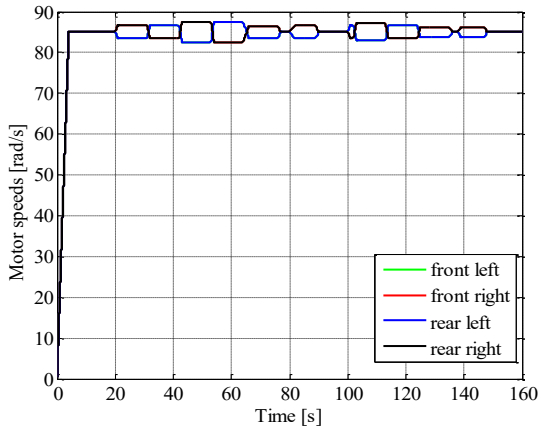

(e) Rotational speed of motors

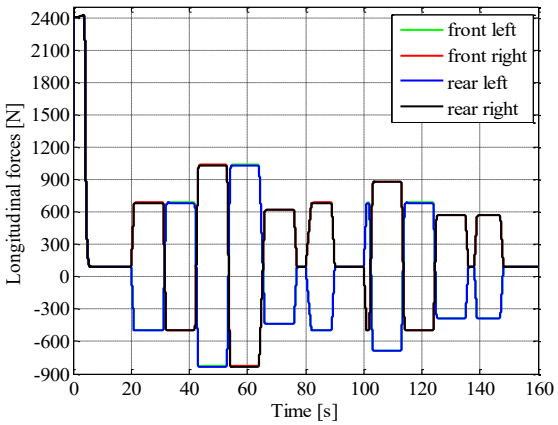

(f) Traction forces

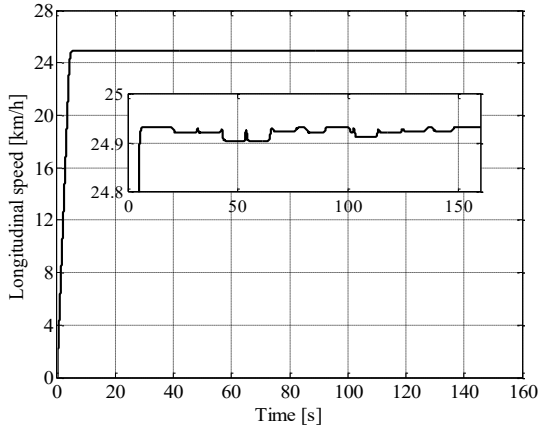

(g) Longitudinal speed

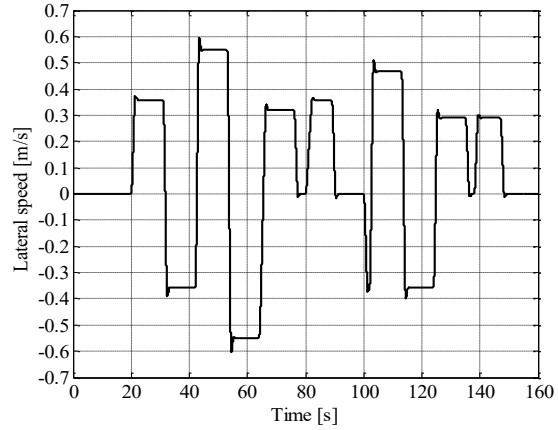

(h) Lateral speed

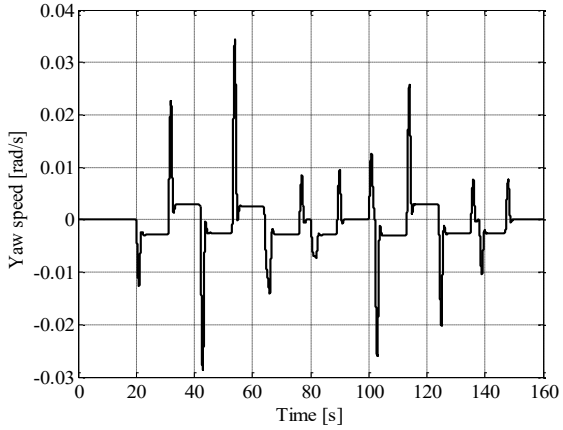

(i) Angular speed

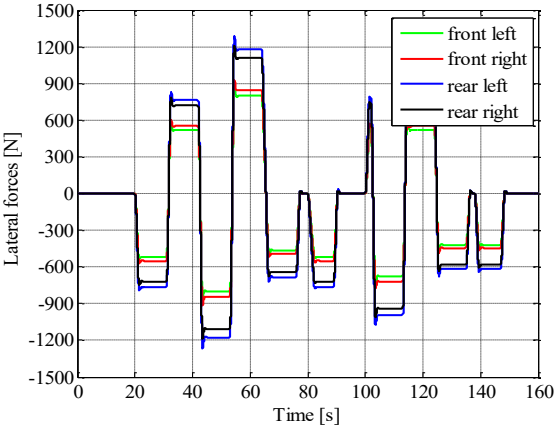

(j) Lateral forces

Figure 4. Simulation results.

CONCLUSION

A 4WD electric vehicle configuration can vary from a single-motor system with a mechanical differential to a quad-motor independent drive setup. The choice depends on performance requirements, cost, and control complexity. Advanced electronic differential systems, inverters, and vehicle control strategies make independent motor

configurations increasingly viable, pushing EVs towards higher efficiency, safety, and stability of the electric vehicle during critical cornering situations. This research investigates a multi-machine control structure designed to enhance the lateral dynamics of an electric vehicle equipped with four PMSM motors, each positioned in the front and rear wheels. The simulation results confirm the effectiveness of the new robust multi-machine control, ensuring that the driving wheel speeds are consistently maintained with strong dynamic and static performance.

REFRENCES

[1] A. Boglietti, A. Cavagnino, D. M. Ionel, M. Popescu, D. A. Staton, and S. J. I. T. o. I. A. Vaschetto, "A general model to predict the iron losses in PWM inverter-fed induction motors," vol. 46, no. 5, pp. 1882-1890, 2010.

[2] G. Y. Sizov, D. M. Ionel, and N. A. J. I. T. o. I. E. Demerdash, "Modeling and parametric design of permanent-magnet AC machines using computationally efficient finite-element analysis," vol. 59, no. 6, pp. 2403-2413, 2011.

[3] S. Choi *et al.*, "Fault diagnosis techniques for permanent magnet AC machine and drives—A review of current state of the art," vol. 4, no. 2, pp. 444-463, 2018.

[4] R. Islam, I. Husain, A. Fardoun, and K. McLaughlin, "Permanent magnet synchronous motor magnet designs with skewing for torque ripple and cogging torque reduction," in *2007 IEEE Industry Applications Annual Meeting*, 2007, pp. 1552-1559: IEEE.

[5] K. Hartani, Y. Miloud, and A. Miloudi, "Improved direct torque control of permanent magnet synchronous electrical vehicle motor with proportional-integral resistance estimator," *Journal of Electrical Engineering and Technology,* vol. 5, no. 3, pp. 451-461, 2010.

[6] A. Abdel-Aziz, M. Elgenedy, and B. J. E. Williams, "Review of switched reluctance motor converters and torque ripple minimisation techniques for electric vehicle applications," vol. 17, no. 13, p. 3263, 2024.

[7] Y. Zhu, M. Yao, and X. J. W. E. V. J. Sun, "A Review on Predictive Control Technology for Switched Reluctance Motor System," vol. 14, no. 8, p. 221, 2023.

[8] A. Hesari, A. Darabi, and F. J. I. E. S. i. T. Pourmirzaei Deylami, "Dual independent rotor axial flux induction motor for electric vehicle applications," vol. 2024, no. 1, p. 5594289, 2024.

[9] H. Abu-Rub, M. Malinowski, and K. Al-Haddad, *Power electronics for renewable energy systems, transportation and industrial applications*. John Wiley & Sons, 2014.

[10] E. M. J. E. Szumska, "Regenerative Braking Systems in Electric Vehicles: A Comprehensive Review of Design, Control Strategies, and Efficiency Challenges," vol. 18, no. 10, p. 2422, 2025.

[11] P. Roy, M. Towhidi, F. Ahmed, S. Mukundan, H. Dhulipati, and N. Kar, "A novel hybrid technique for thermal analysis of permanent magnet synchronous motor used in electric vehicle application," SAE Technical Paper0148-7191, 2020.

[12] N. Murali and S. Ushakumari, "Performance comparison between different rotor configurations of PMSM for EV application," in *2020 IEEE REGION 10 CONFERENCE (TENCON)*, 2020, pp. 1334-1339: IEEE.

[13] W. Liu *et al.*, "A systematic survey of control techniques and applications in connected and automated vehicles," vol. 10, no. 24, pp. 21892-21916, 2023.

[14] R. Rouhani, S. E. Abdollahi, and S. A. Gholamian, "Torque ripple reduction of a synchronous reluctance motor for electric vehicle applications," in *2018 9th Annual Power Electronics, Drives Systems and Technologies Conference (PEDSTC)*, 2018, pp. 386-391: IEEE.

[15] O. D. Aladetola, M. Ouari, Y. Saadi, T. Mesbahi, M. Boukhnifer, and K. H. J. E. Adjallah, "Advanced torque ripple minimization of synchronous reluctance machine for electric vehicle application," vol. 16, no. 6, p. 2701, 2023.

[16] K. Selvam, V. Patel, and S. Sahoo, "Impact of Torque Ripple in PMSM on EV Energy Efficiency and Driving Range," in *2025 International Conference on Sustainable Energy Technologies and Computational Intelligence (SETCOM)*, 2025, pp. 1-6: IEEE.

[17] A. K. Sahoo, R. K. J. A. E. Jena, and E. Engineering, "Improved DTC strategy with fuzzy logic controller for induction motor driven electric vehicle," vol. 6, no. 3, pp. 296-316, 2022.

[18] A. Bouscayrol *et al.*, "Multi-converter multi-machine systems: application for electromechanical drives," *The European Physical Journal-Applied Physics,* vol. 10, no. 2, pp. 131-147, 2000.

[19] S. PROJET *et al.*, "Multimachine Multiconverter Systems for drives: analysis of coupling by a global modeling," in *Proc. of IEEE-IAS anual meeting*, 2000.
[20] A. Bouscayrol *et al.*, "Control structures for Multi-machine Multi-converter Systems with dowstream coupling," 2001.
[21] A. Bouscayrol *et al.*, "Control structures for multi-machine multi-converter systems with upstream coupling," *Mathematics and computers in simulation,* vol. 63, no. 3-5, pp. 261-270, 2003.
[22] K. Hartani and A. Draou, "A new multimachine robust based anti-skid control system for high performance electric vehicle," *Journal of Electrical Engineering and Technology,* vol. 9, no. 1, pp. 214-230, 2014.
[23] C. Direm, K. Hartani, and N. Aouadj, "New Combined Maximum Torque per Ampere-Flux Weakening Control Strategy for Vehicle Propulsion System," *SAE International Journal of Vehicle Dynamics, Stability, and NVH,* vol. 5, no. 10-05-02-0009, 2021.
[24] P. Barrre *et al.*, "Inversion-based control of electromechanical systems using causal graphical descriptions," in *IEEE Industrial Electronics, IECON 2006-32nd Annual Conference on*, 2006, pp. 5276-5281: IEEE.
[25] M. Sekour, K. Hartani, and A. Merah, "Electric Vehicle Longitudinal Stability Control Based on a New Multimachine Nonlinear Model Predictive Direct Torque Control," *Journal of Advanced Transportation,* vol. 2017, 2017.
[26] A. El djallil Rabhi, K. Hartani, Y. Guettaf, and A. Norediene, "Robust Multimachine Control for Bisynchronous Propulsion Traction Chain of an Electric Vehicle," *SAE International Journal of Vehicle Dynamics, Stability, and NVH,* vol. 5, no. 10-05-02-0012, 2021.
[27] K. Hartani, M. Bourahla, Y. Miloud, and M. Sekour, "Electronic differential with direct torque fuzzy control for vehicle propulsion system," *Turkish Journal of Electrical Engineering & Computer Sciences,* vol. 17, no. 1, pp. 21-38, 2009.
[28] K. Hartani, M. Bourahla, and Y. Miloud, "Electronic differential system for an electric vehicle based on direct torque fuzzy control," *INTERNATIONAL REVIEW OF ELECTRICAL ENGINEERING-IREE,* vol. 3, no. 2, pp. 386-394, 2008.
[29] N. Aouadj, K. Hartani, and M. Fatiha, "New Integrated Vehicle Dynamics Control System Based on the Coordination of AFS, DYC, and ED for Improvements in Vehicle Handling and Stability," *SAE International Journal of Vehicle Dynamics, Stability, and NVH,* vol. 4, no. 10-04-02-0009, 2020.
[30] T. Ahmed, H. Kada, and A. Allali, "New DTC strategy of multi-machines single-inverter systems for electric vehicle traction applications," *International Journal of Power Electronics and Drive Systems,* vol. 11, no. 2, p. 641, 2020.